Beam Request for the Proposal No. 125

"The Polarised Charge–Exchange Reaction $\vec{d} + p \to (pp)n$" and Storage cell tests for the polarised target

First results and first determination of the deuteron vector and tensor polarisation at ANKE

A. Kacharava, E. Steffens, S. Yaschenko

Physikalisches Institut II, Universität Erlangen–Nürnberg, 91058 Erlangen, Germany

V.V. Glagolev

Joint Institute for Nuclear Research, Laboratory of High Energy, 141980 Dubna, Russia

D. Chiladze, R. Gebel, K. Grigoriev, V. Hejny, I. Keshelashvili, B. Lorentz, A. Mussgiller, F. Rathmann, R. Schleichert, H. Seyfarth, H. Ströher, A. Wrońska

Institut für Kernphysik, Forschungszentrum Jülich, 52425 Jülich, Germany

S. Dymov, V. Komarov, A. Kulikov, G. Macharashvili, S. Merzliakov, S. Trusov, Yu. Uzikov

Joint Institute for Nuclear Research, LNP, 141980 Dubna, Russia

M. Nioradze

High Energy Physics Institute, Tbilisi State University, 380086 Tbilisi, Georgia

A. Khoukaz, N. Lang, R. Menke, T. Mersmann

Institut für Kernphysik, Universität Münster, 48149 Münster, Germany

H. Rohdjeß

Helmholtz-Institut für Strahlen- und Kernphysik, Universität Bonn 53115, Bonn, Germany

S. Mikirtytchiants

High Energy Physics Department, Petersburg Nuclear Physics Institute, 188350 Gatchina, Russia

C. Wilkin

Physics and Astronomy Department, University College London, London WC1E 6BT, U.K.

for the ANKE Collaboration

Jülich, March 15, 2004

Abstract

from the original proposal No. 125

During our studies of the $pd \to n(pp)$ reaction at ANKE with neutron emission in the backward direction, we have measured two protons at low relative momentum presumably in the $^1S_0$ final state. Now we are exploiting this technique, together with the possibilities offered by the acceleration of polarised deuterons at COSY, to measure the $\vec{d}p \to (pp)_{^1S_0}n$ charge–exchange reaction near the forward direction, i.e. where the four–momentum transfer t between the proton and neutron is small. The data on the differential cross section and analysing power can be interpreted in terms of the amplitudes for the elementary $np \to pn$ charge–exchange process and our results should provide information on the spin–spin terms in the amplitude in the energy range above the existing data of LAMPF (800 MeV) and up to the maximum beam energy per nucleon achievable at COSY (1150 MeV).

Contents

1 Executive Summary

The data analysis from the 50 hours of 1.2 GeV polarised deuteron beam time taken in November 2003 is still far from being complete. Nevertheless, we have achieved the following:

- Measured $\vec{d}p \rightarrow$ single and double-track events in ANKE and clearly identified, amongst others, the $\vec{d}p \rightarrow dp$, $\vec{d}p \rightarrow {}^3\mathrm{He}\,\pi^0$, and $\vec{d}p \rightarrow (pp)n$ reactions;

- Determined the luminosity in the experiment by comparing to published deuteron-proton elastic scattering cross sections, which have a precision of about 10%;

- Obtained differential distributions for the $d\,p \rightarrow (pp)n$ reaction as functions of the momentum transfer t and the pp excitation energy E_{pp};

- Worked with eight different combinations of vector (P_z) and tensor (P_{zz}) deuteron polarisations provided by the ion source and accelerated in COSY;

- Extracted values of P_{zz} by measuring the polarisation dependence of the small angle $\vec{d}p \rightarrow {}^3\mathrm{He}\,\pi^0$ count rates and using the t_{20} analysing power, known with high precision from Saclay measurements;

- Extracted values of P_{zz} by comparing the polarisation dependence of the $\vec{d}p \rightarrow (pp)n$ reaction for small pp excitation energies with the predictions of the undistorted Bugg & Wilkin model, which describes well data published at lower and higher energies;

- Compared our two values of P_{zz} for the six non-zero source spin states with the values obtained before our run by EDDA at lower energies and lower source intensities. Although there is qualitative agreement, the variations for the individual spin states are bigger than expected on the basis of the statistics achieved, suggesting that the systematics of both our and the EDDA measurements must be studied further. Nevertheless the mean value over all states is reasonable: $P_{zz}({}^3\mathrm{He}\pi^0)/P_{zz}(\mathrm{EDDA}) = 0.96 \pm 0.21$, where the error is determined purely from the spread in the individual results;

- Using the values of P_{zz} from the ${}^3\mathrm{He}\,\pi^0$ final state in conjunction with our $\vec{d}p \rightarrow dp$ elastic scattering data, the deduced values of the deuteron vector polarisation P_z are in reasonable agreement with the EDDA values, though again with a spread over different source states that is larger than expected on the basis of statistical errors, which are comparatively small. The mean value is $P_z({}^3\mathrm{He}\pi^0)/P_z(\mathrm{EDDA}) = 1.03 \pm 0.15$.

- Using the measured values of P_{zz} from the $\vec{d}p \rightarrow {}^3\mathrm{He}\,\pi^0$ reaction, we deduce that for the deuteron charge exchange reaction $T_{20} = 0.36 \pm 0.08$, to be compared to the Bugg & Wilkin prediction of 0.42;

The November 2003 data have to be further studied in order to:

- Cross–check with the above described methods by comparing the polarisation and luminosity obtained from the pp quasi–elastic process, which have already been identified with the silicon–telescope system.

- Determine the $(d, 2p)$ absolute cross section to extract individual values of $|\beta(0)|$ and $|\varepsilon(0)|$;

- Investigate the effects of the data cuts on the extraction of the polarisation observables with the aim to reduce the variations apparent for the different spin modes down to the level of the statistics;

- By looking at the ϕ dependence of the cross sections, attempt to derive values of T_{22} for the $\vec{d}p \to {}^3\mathrm{He}\,\pi^0$, and $\vec{d}p \to (pp)n$ reactions. The latter is sensitive to the difference between $|\beta(t)|$ and $|\delta(t)|$ slightly away from the forward direction;

- Identify and measure the analysing powers of other reactions whose final states are seen in the data. These include the low-mass Δ in $\vec{d}p \to (pp)\Delta^0$, the backward $\vec{d}p \to {}^3\mathrm{He}\,\pi^0$, and the $\vec{d}p \to {}^3\mathrm{H}\,\pi^+$ reaction over a wide angular region.

Given the above successes in the first handling deuteron tensor polarisation in internal experiments at COSY, we request to continue our experiment to:

- Determine well the different analysing powers at $T_d = 1.2$ GeV using optimized ion source settings to allow polarimetry for higher energies, using the polarization export technique. The polarimetry will be carried out at $T_d = 1.2$ GeV using both the $p(\vec{d},\,{}^3\mathrm{He})\pi^0$ and $p(\vec{d}, 2p)n$ reaction with the latter having a larger cross section. This can be done using the *Global Jump* procedure, measuring twice at 1.2 GeV with the higher energy sandwiched between. Although, following the Saclay experience, we have no reason to believe that deuterons will suffer significant depolarisation in the COSY ring, this assumption has to be tested with some precision.

- Measure, amongst other reactions, the $p(\vec{d}, 2p)n$ reaction at the three energies of 1.8, 2.0, and 2.2 GeV over an angular range in order to extract values of $|\beta(t)|$, $|\delta(t)|$, and $|\varepsilon(t)|$ in a region where data are essentially absent;

We request one week of beam time per energy for the above study. The 1.8 GeV point will be useful in connection with the ANKE proposal to measure the analysing power in the $p(\vec{d},\,{}^3\mathrm{He})\eta$ reaction near threshold.

However, since the eventual continuation of our programme will involve the measurement of spin-correlation parameters with polarised beams and targets to deduce the relative phases of the *np* charge-exchange amplitudes, we further request one extra week of beam time with an unpolarised target cell to establish that we can achieve the same results with an extended target.

In the following pages we attempt to justify the statements made in this summary.

2 Introduction

The complete description of the NN interaction requires precise data, in particular from double-polarisation experiments [1], for phase–shift analyses (PSA) from which the scattering amplitudes can be reconstructed.

For the pp system such experiments were carried out up to beam energies of about 3.0 GeV [2, 3], whereas much less information is available on spin observables in elastic np scattering, especially above 800 MeV [4, 5]. The PSA results for the isospin $I = 0$ NN system are thus poorly tested experimentally and measurements of any observable at small angles are highly desirable in order to check validity of the PSA solutions for np amplitudes below 40° (c.m.) and, if necessary improve these solutions. The ANKE spectrometer covers angular range $\theta_{c.m.} \sim 0 - 30°$ in the charge-exchange region.

Information on the spin–dependent np elastic amplitudes near the backward direction (the charge–exchange region) can be obtained by measuring the Charge–Exchange (CE) break-up of polarised deuterons on hydrogen. The overall intensity of the spin–dependent parts of the elementary $np \to pn$ CE amplitude can thus be inferred from the probability of the dp CE process. Furthermore, it has been shown [6, 7] that by measuring the deuteron tensor analyzing powers it is possible to separate the intensities of the different spin amplitudes.

Under special kinematic conditions (scattering angle θ close to zero and momentum transfer $t \sim 0$), the dp CE differential cross section is fully determined by the spin–dependent parts of the elementary $np \to pn$ amplitude. A measurement of the differential cross section and the tensor analysing power T_{20} will allow us to extract directly the $|\beta|^2$ and $|\varepsilon|^2$ intensities of the spin amplitudes [8] .

These conditions were realized last year during the COSY machine development week (23-25 November 2003) with a polarised deuteron beam of energy T_d=1.2 GeV (p_d = 2.4 GeV/c). The aim of the run was to carry out a feasibility test of the experiment and to develop the polarimetry of the COSY deuteron beam using ANKE alone, which is very important for future polarisation experiments at COSY and may replace EDDA in the long run.

The preliminary results indicate that we are able to provide good luminosity determination and polarimetry for deuterons, in order to measure the differential cross section and T_{20} of the charge-exchange reaction with reasonable error bars, and thus to reconstruct directly the magnitudes of at least two of the spin-dependent amplitudes with an accuracy sufficient to have an impact upon the nucleon-nucleon data bases. The systematic analysis of the data obtained from the test measurements is currently underway.

3 Experimental set–up

3.1 The Forward Detection System

The experiment was performed at the ANKE spectrometer [9] installed at the internal beam of the COoler SYnchrotron COSY at the Forschungszentrum Jülich. In Fig. 1 those parts of the spectrometer are shown that are relevant for the present experiment. The polarised deuterons stored in the COSY ring ($\approx 3 \times 10^9$ deuterons) impinge on a hydrogen cluster–jet target (thickness $\approx 1 \times 10^{14}$ atoms/cm^2, resulting in a luminosity of $\approx 3 \times 10^{29}$ cm^{-2}s^{-1}).

Two fast protons, emitted in a narrow forward cone with momenta around half that of the deuteron beam, are detected by the Forward detector (FD) system of the ANKE set-up. The detection of proton pairs in the forward direction was already successfully achieved in our proton–induced deuteron break-up experiment [11], which was studied in the region of large momentum transfers.

A silicon telescope system, consisting of three layers of silicon strip detectors [10], is mounted in the target vacuum chamber as a near-target detector.

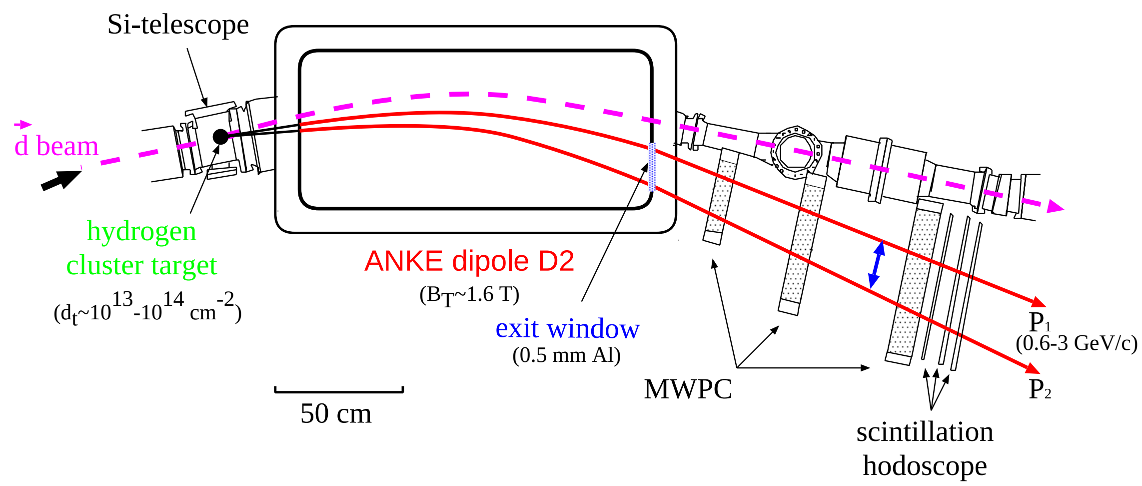

Figure 1: Schematic drawing of the part of ANKE used in the $\vec{d}p \to (pp)_{^1S_0} + n$ experiment

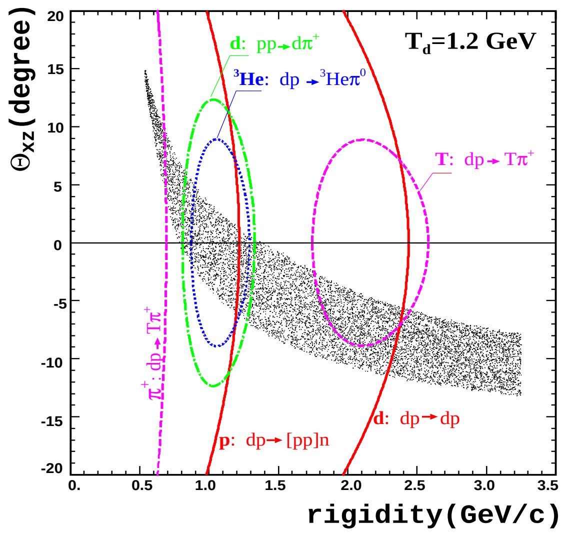

Figure 2: MC simulation of the ANKE acceptance, showing angle *versus* rigidity (p/Z). θ_{xz} is the scattering angle of the emitted particle projected onto the median plane of the spectrometer. The curves show kinematic loci for π^+, p, d, t, and ^{3}He, from the indicated processes. Here $[pp]$ denotes a forward-going proton pair with zero excitation energy.

3.2 Acceptance

The horizontal acceptance of the set–up for $T_d = 1.2$ GeV is shown in Fig. 2, whereas the vertical acceptance corresponds to $\pm 3.5°$. Deuterons from dp elastic scattering falling within the ANKE acceptance are also indicated. These events will be used for both luminosity determination and detector calibration. Also shown are pions and tritons from the $dp \to t\pi^+$ reaction and ^{3}He from the isospin–related $dp \to {}^3\mathrm{He}\,\pi^0$ reaction. Since the tensor analyzing power T_{20} has been well measured for both forward and backward pion production as a function of energy [12], these two reactions can be used as the basis for a polarimeter for the deuteron beam.

A measurement of T_{22} requires us to detect scattering angles away from zero degrees, where this observable vanishes. Making use of the transverse positioning capability of the D2 magnet, the angle interval accepted in the forward detector was optimized for this purpose.

3.3 The COSY deuteron beam

A first test measurement was carried out at the end of November 2003 with the polarised deuteron beam of energy $T_d = 1.2$ GeV.

The experiment used the polarised deuteron beam provided by the COSY ion source. The scheme consists of eight different polarisation states including one unpolarised mixture and seven combinations of vector and tensor polarisations, as shown in Table 1.

Spin Mode	theoretical maximum vector P_z	theoretical maximum tensor P_{zz}	Intensity $[I_0]$
0	0	0	1
1	$-2/3$	0	1
2	$+1/3$	$+1$	1
3	$-1/3$	-1	1
4	$+1/2$	$-1/2$	2/3
5	-1	$+1$	2/3
6	$+1$	$+1$	2/3
7	$-1/2$	$-1/2$	2/3

Table 1: Modes of the polarised deuteron ion source. The intensity modulations between the different modes constitute a compromise in order to achieve higher polarisations. I_0 refers to the maximum number of deuterons delivered by the source and stored in COSY. In our experiment an intensity of $I_0 \approx 3 \times 10^9$ deuterons was achieved.

For each injection into COSY, the polarised ion source was switched to a different polarisation state. The duration of a cycle was sufficiently long (200 s) to ensure stable conditions for the injection of the next state. After the seventh state, the source was reset to the zeroth mode and the pattern repeated. The ANKE data acquisition system received status bits from the source, latched during injection, that ensure the correct identification of the polarisation states during the experiment. Because of their small magnetic moment, deuterons encounter no depolarising resonances in the energy range of COSY and are unlikely to be depolarised. This was recently tested for a vector polarised beam, at least qualitatively, during the SPIN@COSY experiment [13]. It should be noted, that the present experiment is the first one that provides at one and the same time a measurement of both vector and tensor polarisations of the deuteron beam stored in COSY.

4 The data taking

As a first step, for this short test measurement we aimed to take data with the polarised deuteron beam on the unpolarised cluster target. The main trigger (Tr1) for the experiment was a coincidence in the forward hodoscope. In parallel the trigger from the silicon telescope alone has been used (Tr2), in order to have the possibility of identifying quasi-elastic *pp* scattering for the deuteron vector polarisation measurements. A special trigger (Tr3), based on energy loss in the forward hodoscope, was used to identify ^{3}He particles to select events from the polarimetry reaction $\vec{d}p \to {}^3\text{He}\,\pi^0$.

The Beam Current signal (BCT) was fed into a voltage–to–frequency converter at the EDDA electronics, transformed into an optical signal to avoid signal deterioration, sent over to ANKE, where it was fed, after conversion back to a NIM–signal, into the ANKE scaler system. Thereby the BCT signal becomes available in the normal ANKE data stream.

As one example of the experimental conditions, the ratio of L/BCT is shown in Fig. 3 for the spin-mode zero (unpolarised beam), where the L denotes the Luminosity, determined in this experiment with an accuracy of about 10% (see the next section) and BCT signal, known to about 1%. This ratio contains the information about the target behavior run by run.

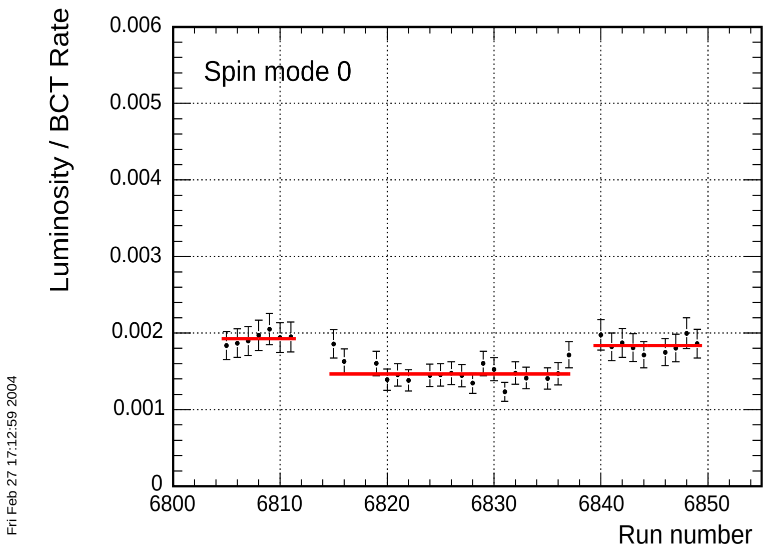

Figure 3: Target 'oscillation' run by run.

5 The data processing

5.1 Luminosity determination

The luminosity for all the runs was evaluated using *dp* elastic scattering with a single deuteron registered in the Forward Detector at the small scattering angles in the laboratory system of 4° to 10° (see Fig. 2). Because this process has a large cross section and is not suppressed much by the acceptance of set-up, it is very clear in the momentum and angle–momentum spectra, and is thus easily selected.

Deuterons from the spin-zero mode events (unpolarised beam) were analyzed in one degree bins in polar angle intervals in the range $4^\circ - 10^\circ$. The acceptance was calculated using a GEANT-based simulation program that includes a realistic description of the set-up. In view of the dependence of acceptance on θ_{lab}, we concentrated on the region of $\theta_{lab} = 5.5^\circ - 9^\circ$, where the acceptance changes smoothly.

The elastic peak region in the momentum spectrum of the single track events (see left panel of Fig. 4) was fitted by the sum of a Gaussian and linear function, and events were selected within 3σ from the fitted average momentum value. In the right panel of Fig. 4 an example of such a fit is shown.

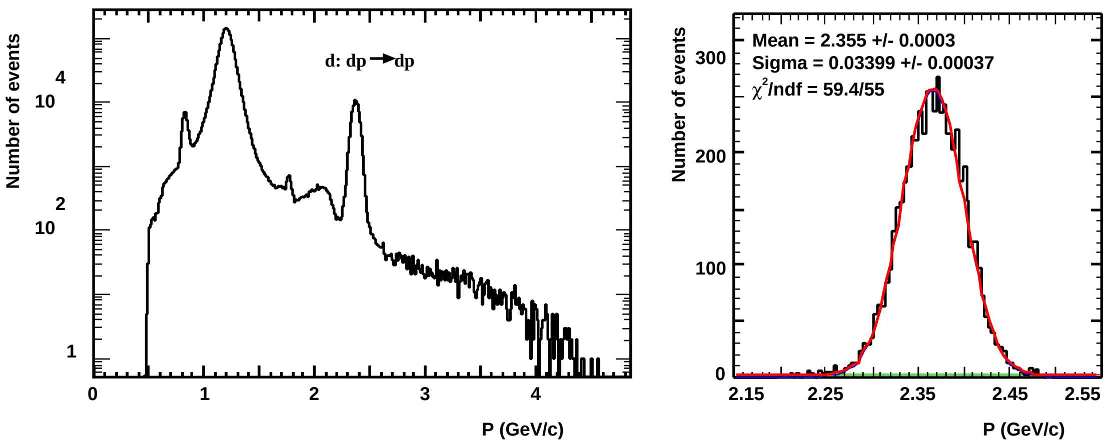

Figure 4: Left panel: Single-track momentum spectrum for the *dp* data with a deuteron beam of 2.40 GeV/c. Right panel: Fit result of the elastic peak region with the sum of a Gaussian and linear function.

After correction of the counts for the dead-time and acceptance, the luminosity of the different polar angle bins was calculated. The weak dependence of luminosity on polar angle is shown in Fig. 5. By averaging the luminosity over the polar angle mean values are obtained. The errors correspond to a root mean squared deviations of the luminosities, determined for individual angular bins. These errors were considered as one source of systematic uncertainties.

These luminosity evaluations depend, of course, on knowledge of the *dp* elastic cross section at this energy and so a second source of uncertainty is the accuracy of the input cross section. The *dp* total, inelastic, and elastic total and differential cross sections have been measured at 10 momenta in the range $2.0 - 3.7$ GeV/c [14]. The slope parameters of the forward portions of the differential cross sections were measured to about 5% at all momenta.

From fits to these data we found a function to describe the differential cross section at $p_d = 2.40$ GeV/c in our angular interval. This is shown as the red line in Fig. 6, together with experimental data [14] at $p_d = 2.46$ GeV/c. A second source of error is thus the luminosity determination, estimated to be about $\approx 8\%$ (see solid blue line corridor).

In parallel to the charge-exchange break-up and *dp* elastic scattering, we detect quasi-

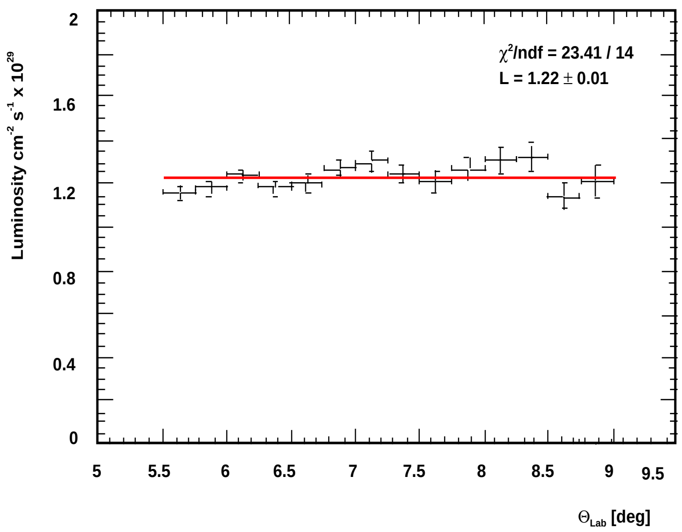

Figure 5: Angular dependence of the luminosity determined for dp forward scattering for single run. The error bars are purely statistical.

free pp scattering using the silicon telescope system placed close to the target region in coincidence with the Forward Detection system. This reaction, which will eventually be used for the measurement of the vector polarisation component of the deuteron beam, can also be considered as an additional reaction for checking the cross section normalization.

5.2 Identification of polarimetry reactions

The deuteron vector polarisation can be measured by analyzing the azimuthal asymmetry of the fast protons from quasi–free proton scattering on the hydrogen target. For an unpolarised target, the $\vec{d}p \to (pn)p$ quasi–free analysing power is known from measurements of pp elastic scattering [15], and can be identified well using the ANKE spectator detector (silicon telescope). A similar method was already used at JINR Dubna [17] and at Saturne [18].

The differential cross section and tensor analysing power T_{20} for the $\vec{d}p \to {}^3\mathrm{He}\,\pi^0$ channel have been measured in the forward and backward c.m. directions at 19 energies between 0.5 and 2.2 GeV at Saturne [12]. The measured value of the T_{20} which we are using in the P_{zz} estimation for our beam energy (T_d=1.2 GeV), was determined in [12] with good accuracy ($\sim 2\%$):

$$T_{20} = -0.661 \pm 0.0157 \,.$$

Furthermore, the angular distributions of the vector (A_y) and tensor (A_{yy}) analysing powers of $\vec{d}p$ elastic scattering were measured at SATURNE at 1.2 GeV, in the range including forward angles ($\theta_{cm} = 32^\circ - 180^\circ$) [19].

The values of the A_y and A_{yy} that we are using in the P_z estimation were also well measured in [19] over our angular range:

$$\begin{aligned} A_y(9.5^\circ) &= 0.427 \pm 0.013 \\ A_{yy}(9.5^\circ) &= 0.647 \pm 0.029 \,. \end{aligned}$$

These two reactions have large enough cross sections to allow them to be detected with good statistical accuracy.

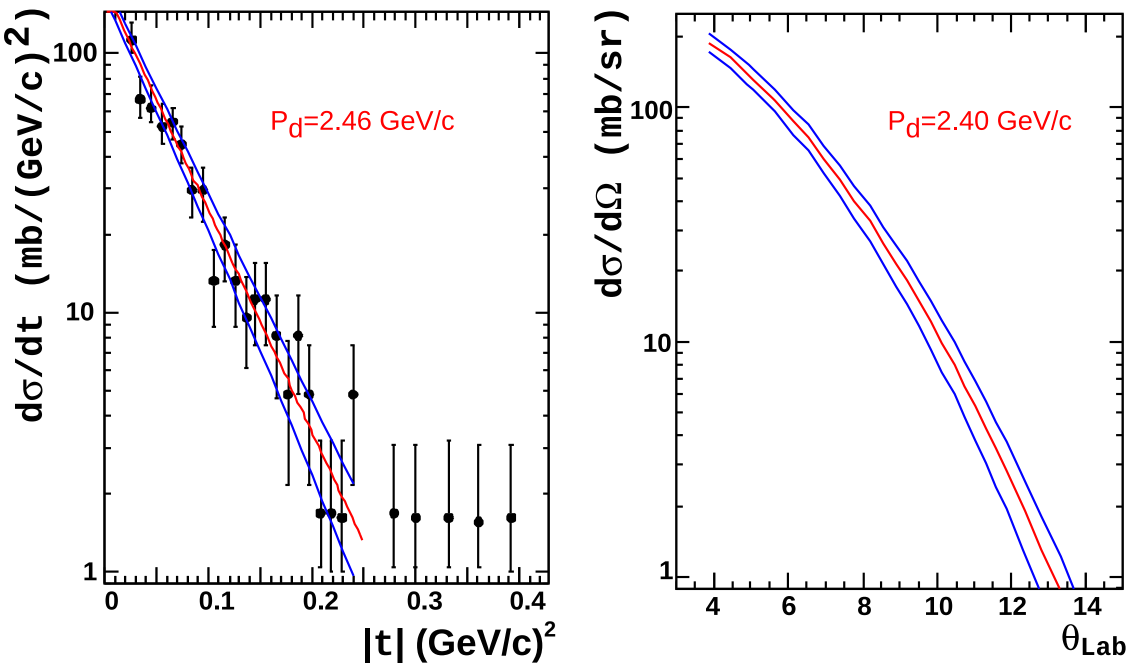

Figure 6: The invariant elastic differential cross section at p_d=2.46 GeV/c from experiment [14] (left panel). The lab differential cross section recalculated from these data at p_d=2.40 GeV/c is shown in the right panel as a red line.

In the reaction $dp \to {}^3\text{He}\,\pi^0$ two particles are produced, one neutral and one of charge two and so the π^0 is identified through the missing mass using only the ^{3}He information. The preliminary result for the isolation of this reaction is shown in Fig. 7. The high momentum branch of ^{3}He particles was identified well by off-line analysis applying two-dimensional cuts in ΔE *versus* momentum and Δt *versus* momentum for individual layers of the forward hodoscope (an additional layer of the sidewall hodoscope was used behind the forward hodoscope). Though the peak in Fig. 7 is wide, this is not critical since, apart from the radiative capture, there is no physical background over this region.

Therefore, using the processes $dp \to {}^3\text{He}\,\pi^0$ (for the P_{zz} measurement), $dp \to dp$ (for the P_z and P_{zz} measurement), and quasi-free pp scattering (for the cross checking of P_z measurement), a simultaneous calibration of the vector and tensor components of polarised deuteron beam at COSY becomes possible for the first time.

5.3 Beam polarisation determination

5.3.1 The measurement of $\mathbf{P_{zz}}$ using the reaction $\vec{\mathrm{d}}\mathrm{p} \to {}^3\mathrm{He}\,\pi^0$

The differential cross section for the polarised deuteron beam can be expressed in the following form [20]:

$$\frac{d\sigma^{\uparrow}}{d\Omega}(\vartheta,\varphi) = \frac{d\sigma_{\circ}}{d\Omega}(\vartheta)\left\{1+\frac{3}{2}P_zA_y(\vartheta)\cos\varphi+\frac{1}{4}P_{zz}[A_{yy}(\vartheta)(1+\cos 2\varphi)+A_{xx}(\vartheta)(1-\cos 2\varphi)]\right\}$$

For the case of $\vartheta \approx 0^\circ$, and assuming that $\cos 2\varphi = 1$, we get:

$$\frac{d\sigma^{\uparrow}}{d\Omega}(\vartheta,\varphi) = \frac{d\sigma_{\circ}}{d\Omega}(\vartheta)\ \left\{1+\tfrac{1}{2}P_{zz}A_{yy}(\vartheta)\right\}\ ,$$

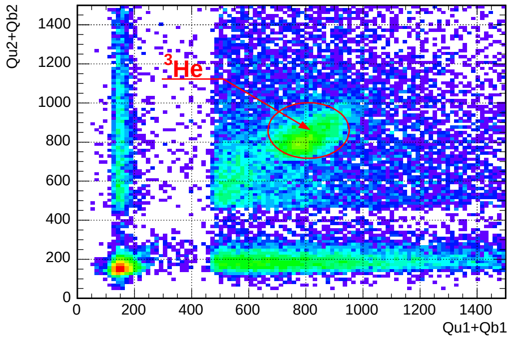

(a) ^{3}He identification

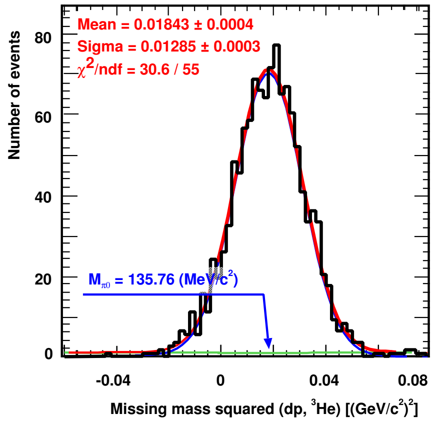

(b) Missing mass squared for the reaction $dp \to {}^3\mathrm{He}\,X$. The result of the peak fit is indicated.

Figure 7: Identification of the $dp \to {}^3\mathrm{He}\,\pi^0$ reaction.

where, for $\vartheta = 0^\circ$, $A_{yy} = -\sqrt{2}\,T_{20}$. Finally the deuteron beam tensor polarisation (P_{zz}) is obtained from the known tensor analysing power (T_{20}) as:

$$P_{zz} = \frac{2\sqrt{2}}{T_{20}} \left[\frac{d\sigma_\circ}{d\Omega}(\vartheta) - \frac{d\sigma^\uparrow}{d\Omega}(\vartheta) \right] \Big/ \frac{d\sigma_\circ}{d\Omega}(\vartheta)\,.$$

For each of the spin modes of the COSY beam we identify the polarimetry reaction run by run using the missing-mass technique. The mean value for the reconstructed pion mass was close to $M_{\pi^0} = 135.4 \pm 3$ MeV/c^2 for all runs. The background was less than 4% and stable. After the correction of the counts in a $\pm 2.5\,\sigma$ range of missing mass (around 150-200 events for each spin mode in a 1° interval of the ^{3}He particles) on the dead-time (which is different for each spin mode) and normalizing them on the BCT signals, we calculate the P_{zz} value assuming that we are selecting polarimetry reaction at zero degrees and that $P_z \approx 0$. The results for the P_{zz} measurement for each run are shown in Fig. 8 and the average values for each spin mode in Table 2.

5.4 The measurement of $\mathbf{P_z}$ using the reaction $\vec{\mathbf{d}}\mathbf{p} \to \mathbf{dp}$

Based on the known form of the differential cross section [20], and assuming that ANKE acceptance of the azimuthal angle is around 180 degree, which means that $\cos 2\varphi \approx 1$ and $\cos\varphi \approx -1$, we obtain the following expression for P_z:

$$P_z = \frac{2(\frac{d\sigma^\uparrow}{d\Omega}(\vartheta) - \frac{d\sigma_\circ}{d\Omega}(\vartheta)) - \frac{d\sigma_\circ}{d\Omega}(\vartheta)P_{zz}A_{yy}}{3\frac{d\sigma_\circ}{d\Omega}(\vartheta)A_y < \cos\varphi >}\,,$$

where the values of A_y and A_{yy} are known [19].

The results of the Pz measurement for each run with the same method used for P_{zz} measurements are shown in Fig. 9 with the averaged values per source state being given in Table 3.

Spin Mode	P_{zz} (^{3}He π^0)	P_{zz} (ppn)	P_{zz} (EDDA)	P_{zz} (ideal)
1	-0.019 ± 0.096	-0.017 ± 0.056	0.057 ± 0.051	0.000
2	0.466 ± 0.106	0.570 ± 0.053	0.594 ± 0.050	1.000
3	-0.656 ± 0.081	-0.409 ± 0.054	-0.634 ± 0.051	-1.000
4	-0.106 ± 0.071	-0.216 ± 0.042	-0.282 ± 0.052	-0.500
5	0.604 ± 0.079	0.567 ± 0.039	0.537 ± 0.052	1.000
6	0.679 ± 0.081	0.619 ± 0.040	0.545 ± 0.050	1.000
7	-0.346 ± 0.069	-0.150 ± 0.042	-0.404 ± 0.053	-0.500

Table 2: Average values of P_{zz} obtained from the EDDA measurements prior to our experiment at lower energies and intensities compared with the values obtained from our $\vec{d}p \to (pp)n$ and $\vec{d}p \to {}^3\text{He}\,\pi^0$ measurements.

Spin Mode	P_z (P_{zz} from ^{3}He π^0)	P_z (P_{zz} from ppn)	P_z (P_{zz} from EDDA)	P_z (ideal)
1	-0.535 ± 0.023	-0.535 ± 0.022	-0.499 ± 0.021	-0.667
2	0.170 ± 0.021	0.219 ± 0.019	0.290 ± 0.023	0.333
3	-0.299 ± 0.018	-0.172 ± 0.017	-0.248 ± 0.021	-0.333
4	0.408 ± 0.012	0.351 ± 0.011	0.381 ± 0.022	0.500
5	-0.582 ± 0.019	-0.602 ± 0.018	-0.682 ± 0.022	-1.000
6	0.722 ± 0.013	0.692 ± 0.011	0.764 ± 0.022	1.000
7	-0.331 ± 0.015	-0.232 ± 0.014	-0.349 ± 0.022	-0.500

Table 3: Average values of P_z obtained from the EDDA measurements prior to our experiment at lower energies and intensities. These are compared to the values obtained from the $\vec{d}p \to dp$ reaction using the values of P_{zz} deduced from our $\vec{d}p \to (pp)n$ and $\vec{d}p \to {}^3\text{He}\,\pi^0$ measurements.

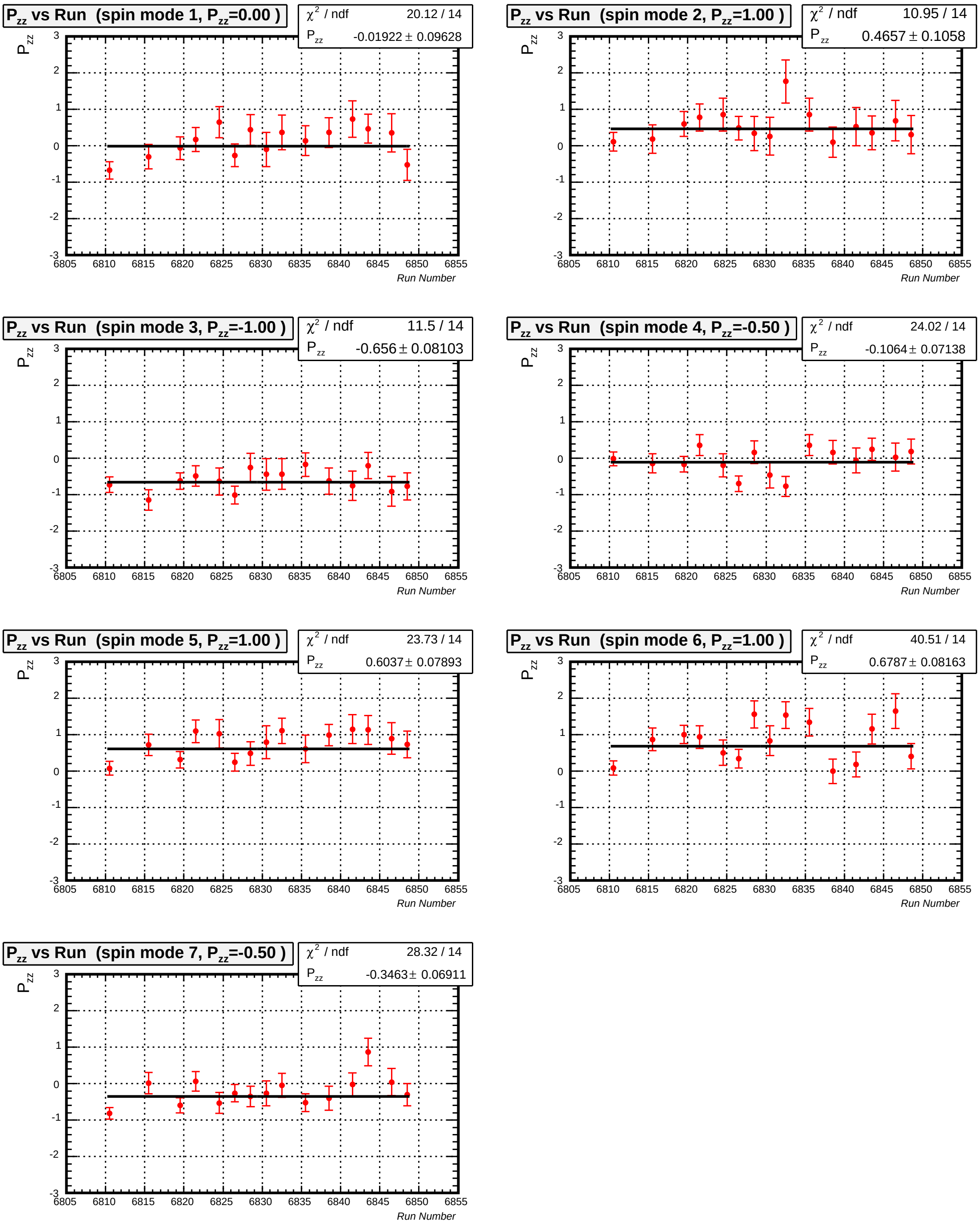

Figure 8: The result of P_{zz} measurement run by run in November 2003 beam time using $\vec{d}p \to {}^3\mathrm{He}\,\pi^0$ reaction.

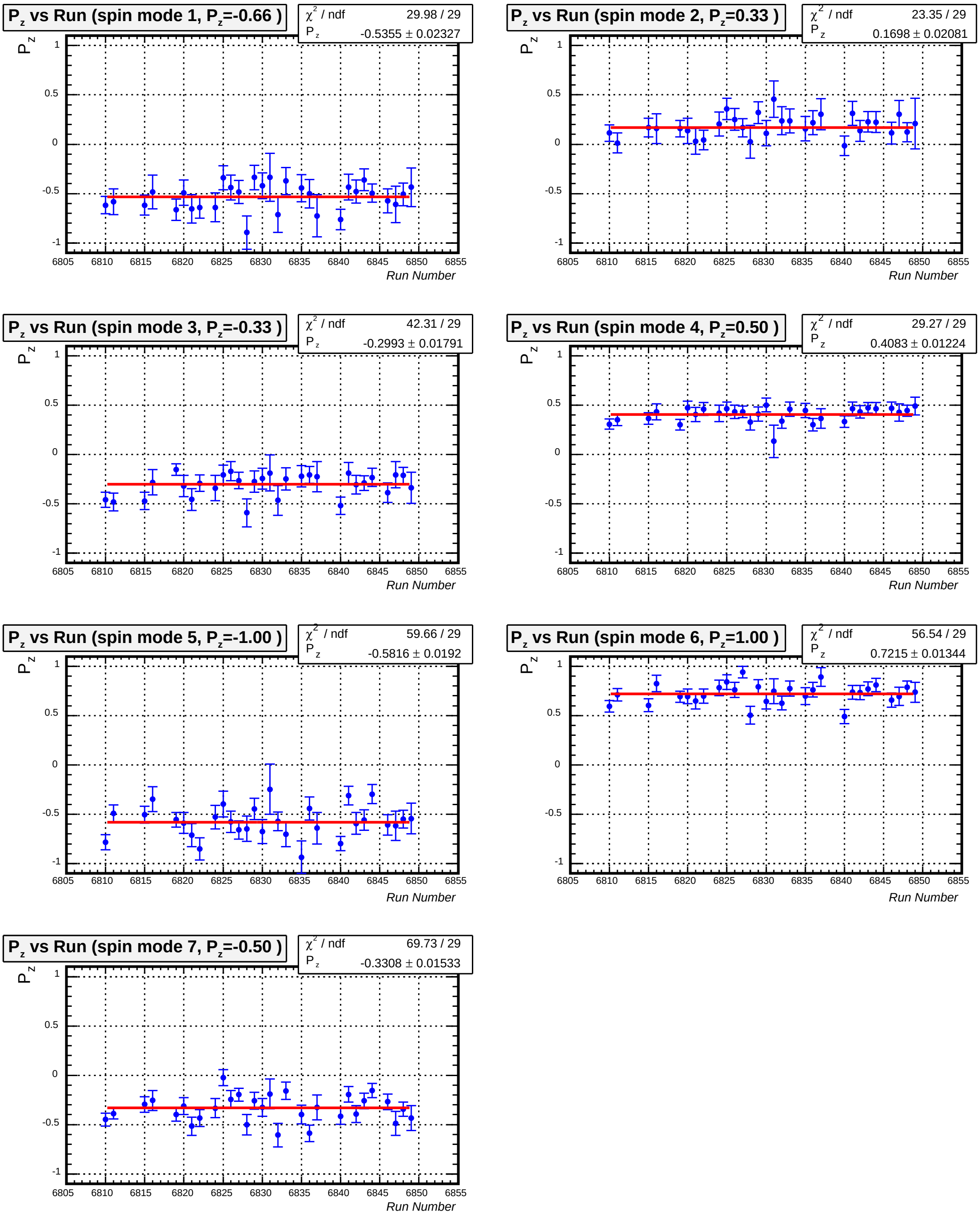

Figure 9: The result of P_z measurement run by run in November 2003 beam time using $\vec{d}p \to dp$ reaction.

5.5 Charge-exchange break-up

The first step in processing the dp break-up data is to choose two-track events using the MWPC information. The known magnetic field map of D2 allowed us to reconstruct the three-momentum as well as the track length for each track. Proton pairs were then selected in arrays of two-particle events by comparing the difference Δt_{mt} between arrival times registered in the hodoscope with a similar difference Δt_{tof} estimated from the reconstructed track length and momenta [11].

The break-up process was identified from the missing-mass with respect to the observed proton pairs (see Fig. 10). The spectra for all spin modes reveal a well defined peak at M_{miss} equal to the neutron mass to within 1%; the mean value for the reconstructed neutron mass is $M_n = 939.9 \pm 2$ MeV/c^2. The background was less than 2% and stable so that the charge-exchange process was identified with high accuracy.

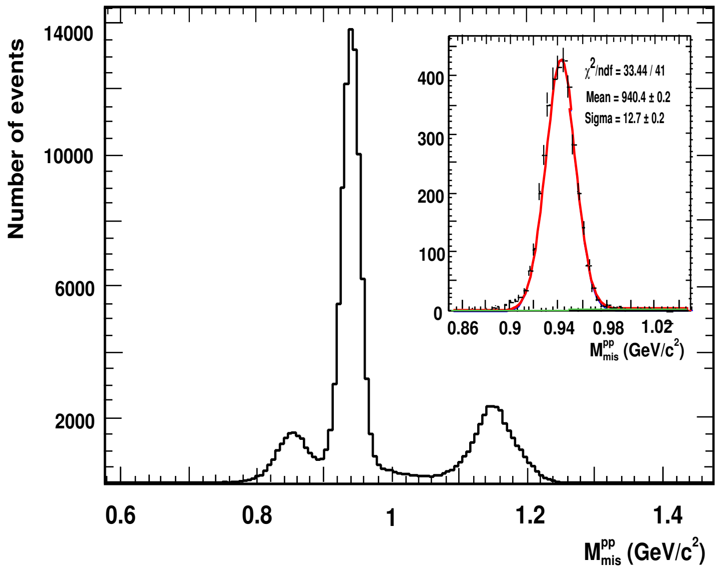

Figure 10: Missing mass distribution of all observed proton pairs. The inset shows the distribution near the neutron mass for the pairs selected by the time-of-flight difference.

5.6 The measurement of T_{20} for the $\vec{\mathbf{d}}\mathbf{p} \to (\mathbf{pp})_{^1\mathbf{S}_0} + \mathbf{n}$ charge-exchange reaction

The method and assumptions are similar to those used for the P_{zz} calculation (see Sec. 5.3). The counts belonging to the $\vec{d}p \to (pp)_{^1S_0} + n$ reaction with the final proton pair produced near zero degrees with small excitation energy ($E_{pp} < 2$ MeV) were identified. Taking the beam tensor polarisation (P_{zz}) determined from the polarimetry reaction, we can use the ratios of the number of events recorded for different spin states of the beam. The final expression used for the T_{20} determination (assuming that the T_{22} tensor analysing power is small), can be written in the form:

$$T_{20} = \frac{2\sqrt{2}}{P_{zz}} \left[\frac{d\sigma_\circ}{d\Omega}(\vartheta) - \frac{d\sigma^\uparrow}{d\Omega}(\vartheta) \right] \Big/ \frac{d\sigma_\circ}{d\Omega}(\vartheta) \, .$$

Using the extracted counts of the $\vec{d}p \to (pp)_{^1S_0} + n$ reaction normalized to the BCT counts, we get the results for T_{20} run by run that are shown in Fig. 11.

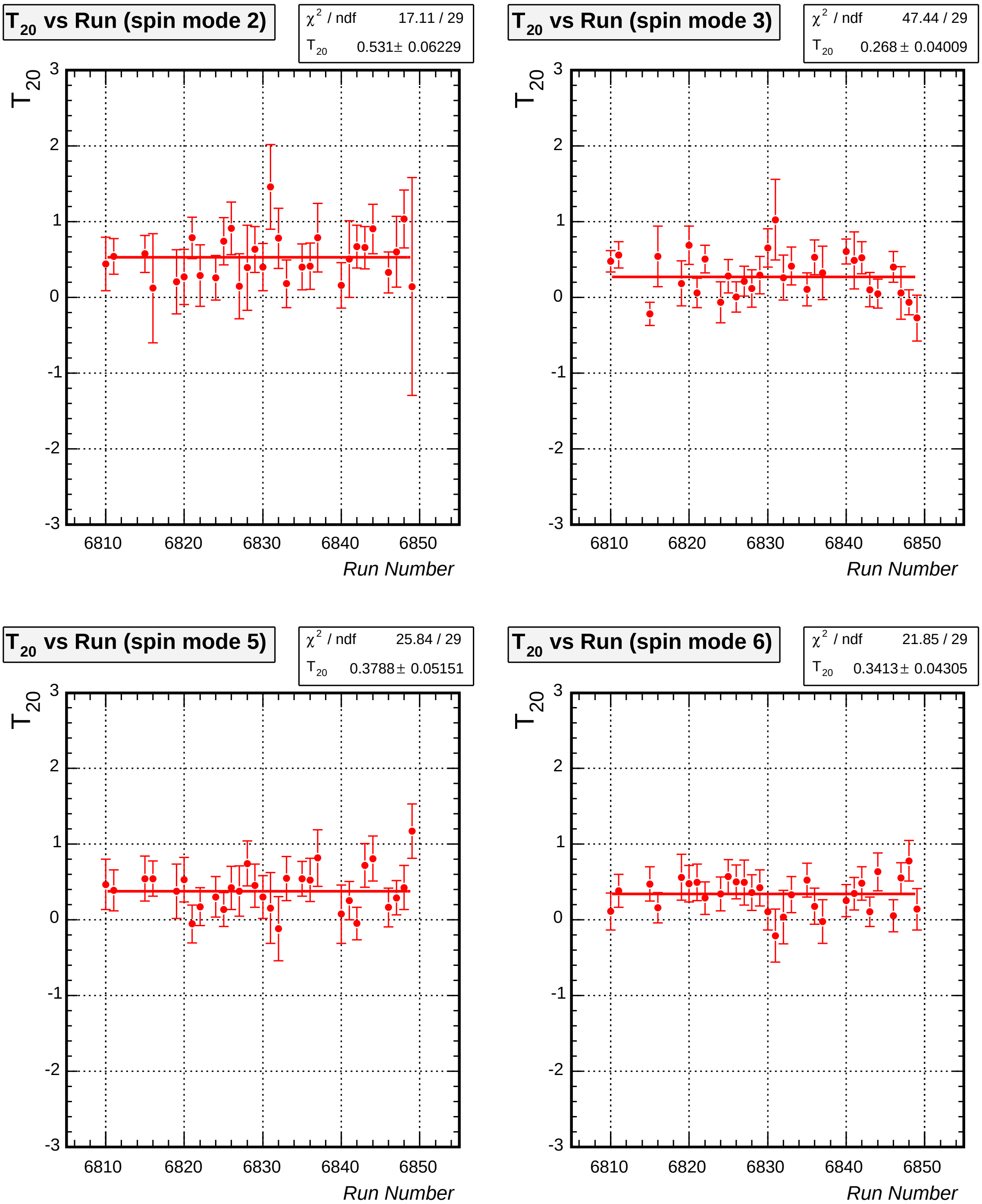

Figure 11: Results of the T_{20} measurement for the $\vec{d}p \to (pp)_{^1S_0} + n$ charge-exchange reaction.

5.7 Differential cross section

The determination of the cross section requires us to take into account corrections for the MWPC efficiency and FD acceptance for detecting the proton pair. These two procedure are now in progress.

The event distribution in the four-momentum transfer t between the proton and neutron is shown on the left panel of Fig. 12 while the right panel shows the histogram of E_{pp} events. The different colors on the histograms show events with sequentially the conditions $\theta_{pp} < 5^\circ, 4^\circ, 3^\circ, 2^\circ$. The shape of the dN/dt distribution is typical for the np charge-exchange process [21, 22].

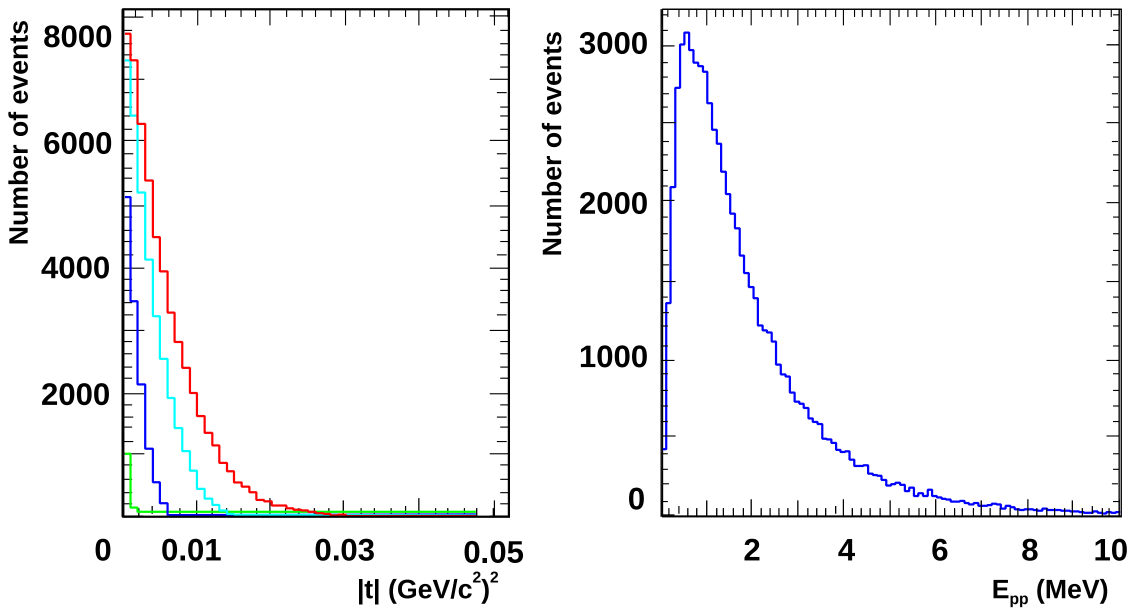

Figure 12: The momentum transfer t and excitation energy E_{pp} distributions for the $\vec{d}p \to (pp)n$ charge-exchange reaction.

The distribution in the distances between hits by the proton pairs ($E_{pp} < 3$ MeV) in the MWPCs has an rms value of 3.0 cm. The loss of pp pairs due to the two tracks being too close should therefore only be significant for $E_{pp} < 0.3$ MeV. Since a resolution of 0.2 (0.3) MeV at $E_{pp} = 0.5(3)$ MeV has been achieved [11], proton pairs with $E_{pp} < 3$ MeV could be reliably selected.

6 Spin-dependent amplitudes

In Fig. 13 are shown the values of the moduli of the two forward spin-flip amplitudes, as functions of energy, taken from the current prediction of the SAID data base [25]. In the intermediate energy range these predictions have changed little since the estimates of Bugg & Wilkin [7] because few experiments have been carried out in this region.

We have measured the $\vec{d}p \to ppn$ differential cross section with a statistical accuracy of better than 3%. This is much smaller than the uncertainty in the absolute normalization derived from the published dp elastic scattering data, which is on the 8% level [14]. In impulse approximation the forward differential cross section is proportional to $2|\beta(0)|^2 + |\varepsilon(0)|^2$ times form factors. However, before we can use this, we must first study more carefully the acceptance in the pp excitation energy because the form factors are sensitive

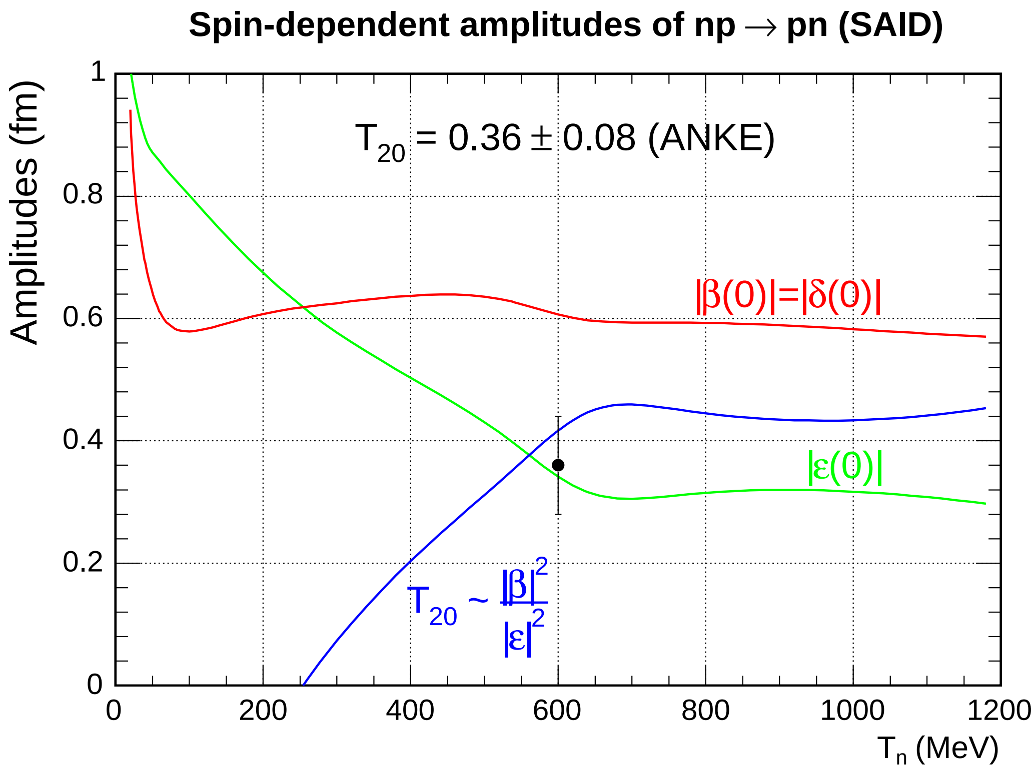

Figure 13: Predictions for the moduli of the two independent $np \to pn$ scattering amplitudes at $t = 0$, taken from the SAID database [25], along with the associated prediction of T_{20} for $\vec{d}p \to (pp)_{^1S_0}n$ in impulse approximation. The latter is compared to our very preliminary point of $T_{20} = 0.36 \pm 0.08$ at $\frac{1}{2}T_d = 600$ MeV.

functions of E_{pp} [7]. Nevertheless, in the region $E_{pp} \leq 2$ MeV, the final pp system is essentially pure S-wave and the acceptance corrections largely cancel out for the analysing powers. Thus, in the forward direction,

$$T_{20} = \sqrt{2}\left(\frac{|\beta(0)|^2 - |\varepsilon(0)|^2}{2|\beta(0)|^2 + |\varepsilon(0)|^2}\right),$$

which means that the ratio of the two forward spin-dependent $np \to pn$ amplitudes can already be deduced from our preliminary results using

$$\frac{|\beta(0)|^2}{|\varepsilon(0)|^2} = \left(\frac{1 + T_{20}/\sqrt{2}}{1 - \sqrt{2}\,T_{20}}\right).$$

The energy dependence of the predicted T_{20} using the SAID input is also shown in Fig. 13 along with our value of $T_{20} = 0.36 \pm 0.08$. Alternatively, using this value, we obtain

$$\frac{|\beta(0)|}{|\varepsilon(0)|} = 1.60 \pm 0.25\,.$$

to be compared to the SAID prediction of 1.79 [25].

7 Polarised gas–target: Cell tests

Although the current proposal will be carried out with the hydrogen cluster target, the $\vec{d}\vec{p}$ spin–correlation studies envisaged in the continuation necessitate the availability of a polarised hydrogen target. A polarised storage cell gas target is being developed at IKP in collaboration with the St. Petersburg Nuclear Physics Institute, the Friedrich–Alexander–Universität Erlangen–Nürnberg, and the Universität zu Köln. A beam of polarised hydrogen (or deuterium) atoms from an atomic beam source (ABS) [23] will feed an open–ended storage cell. The polarisation axis of the atoms is given by the axis of quantitation in the vertical stray field of the spectrometer magnet D2. Transverse deuteron–beam and proton–target polarisation will allow us to study the reactions discussed in the original proposal [8]. A full amplitude determination requires longitudinally polarised protons in the target, which means developing an appropriate magnetic holding field at the polarised gas–target storage cell. The necessary homogeneous field has to extend over the full cell–tube length of about 40 cm. These difficult tasks require magnetic field calculations with use of, *e.g.* the MAFIA code during the design phase in order to optimize and complete a tentative first lay–out [24]. The field–shaping system has then to be built, installed and commissioned at ANKE. Some test measurements necessary for the target design have already been undertaken at COSY.

7.1 Motivation for the cell tests

The goal of the cell test was to estimate the beam size at the ANKE target position since, before these tests, the size of the COSY beam at injection and after acceleration was very uncertain. These findings are needed to build the storage cells for the polarised target and, depending on the size of the cells, determine how much beam will be lost at injection, and also determine the target density.

7.2 Description of experimental equipment and measurement procedure

For these tests an aluminum aperture with inner size 50×25 mm and 3 mm walls was constructed. The inner size is larger than the expected size of the beam at injection so that the aperture does not touch the beam, provided that it is well centered. In order to move the aperture horizontally and vertically, the XY-table shown in Fig. 14 was build with a frame supporting a number of different apertures. The proton beam enters from the lower left side. The XY-table was mounted from the left side of the target chamber. As shown in Fig. 14, the set-up was built with due consideration to the other installed devices. The stepping motors of the XY-table have to be very precise, with the maximum error in a step being $50\,\mu$m. The frame and its support can be moved out from the beam to make sure that beam does not touch any of the apertures, when data taking takes place at ANKE for other experiments. The dimensions of the large aperture are shown in Fig. 15.

The COSY accelerator crew stabilized the beam in the center of the aperture before the accelerated beam tests and the shaded area in Fig. 15 is the assumed proton beam size at injection.

An injection takes 15 seconds and, since each cycle lasts 600 seconds, we could measure 10 points with a time delay of about one minute. All 10 points were taken at a single frame position, which was moved from the central position only after the beam was injected and accelerated.

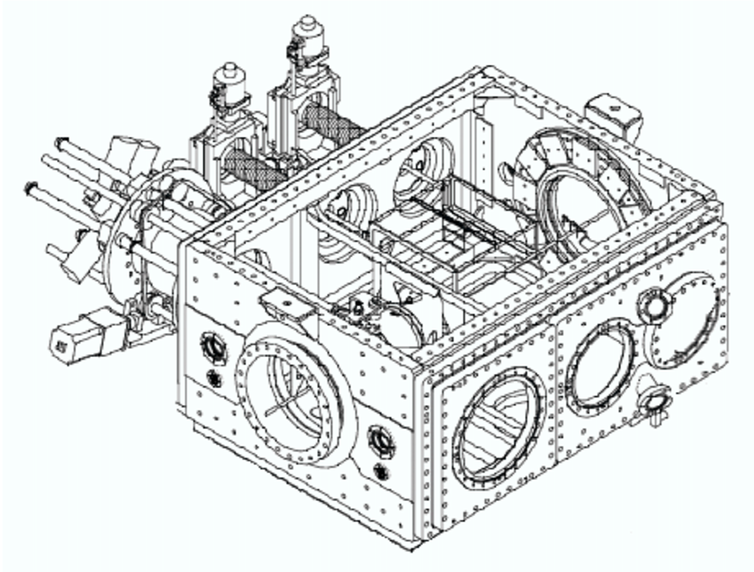

Figure 14: The XY-table with frame at ANKE

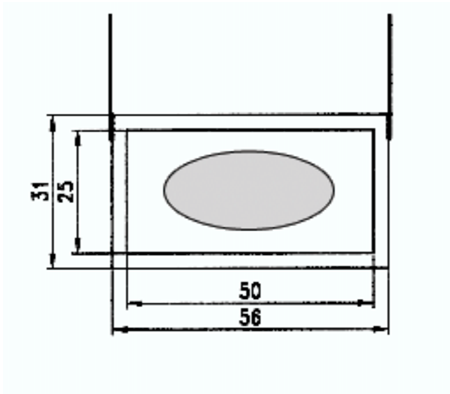

Figure 15: Aperture with the beam

7.3 Results

The results of these tests, illustrated in Fig. 16, show that there are a few millimeters of 0% loss of the beam intensity, which means that at the center of our aperture we did not cut the beam. The shaded areas in the following figures are measured regions where the proton beam at injection and during acceleration touch the aperture walls (Fig. 16). An estimate for the beam diameter is given by the sum of the shaded areas.

After we have calculated the real position of the beam center we estimate the radius of the beam in both directions. As illustrated in Fig. 17, without a target we have beam shape that is close to circular, with dimensions 8 mm $\times$ 10 mm.

Using MAD, the β-functions for the X and Y axes of the beam were calculated. The comparison of the program results with the measurements is given in Table. 4.

The beam sizes were derived from the β-functions

$$X = \sqrt{\beta_x A_x^{max}}; \quad Y = \sqrt{\beta_y A_y^{max}}$$

where $A_x^{max} \approx 120\,\mu$m and $A_y^{max} \approx 25\,\mu$m.

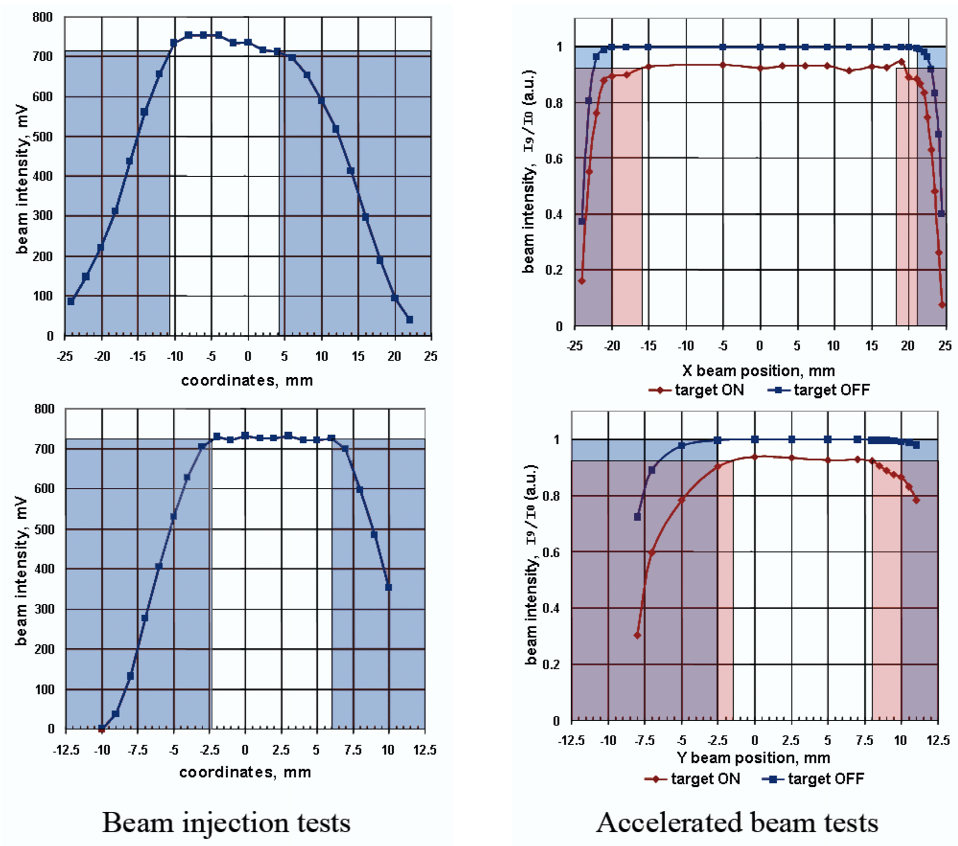

Figure 16: Results of the aperture tests at injection and after acceleration

	Injection		Acceleration	
Axis	β function	measurements	β function	measurements
X [mm]	36	40	37	8
Y [mm]	16.5	20	18	10

Table 4: Diameter of the beam.

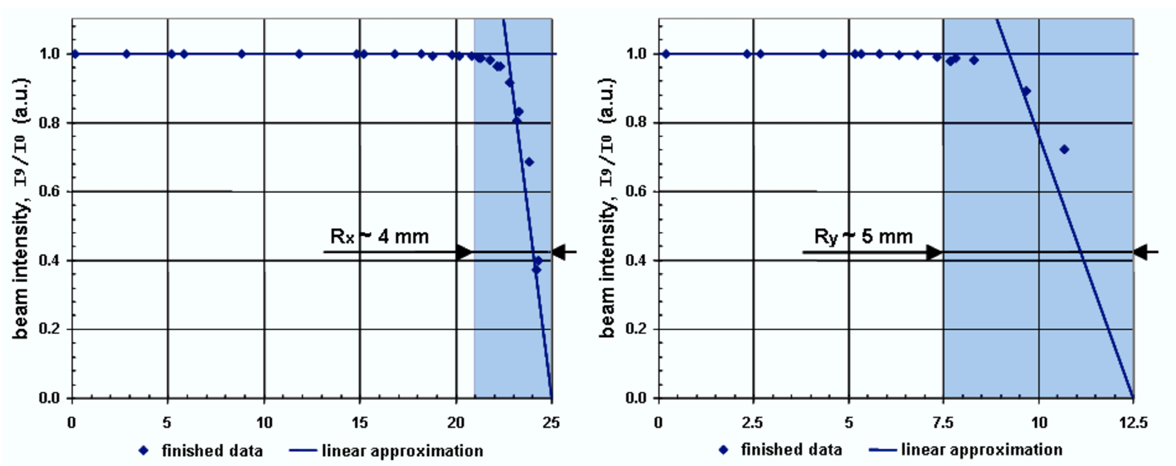

Figure 17: X beam position – target OFF, Y beam position – target OFF

7.4 Test measurement using the storage cell with an unpolarised gas inlet.

The next step before the measurements with polarised protons or deuterons should be a measurement using the storage cell with an unpolarised gas inlet and, for such tests, we will build a rectangular cell with a gas inlet. We can assume that the beam size with an unpolarised gas target has a linear dependence on the target density and the size of the new cell could be designed on this basis.

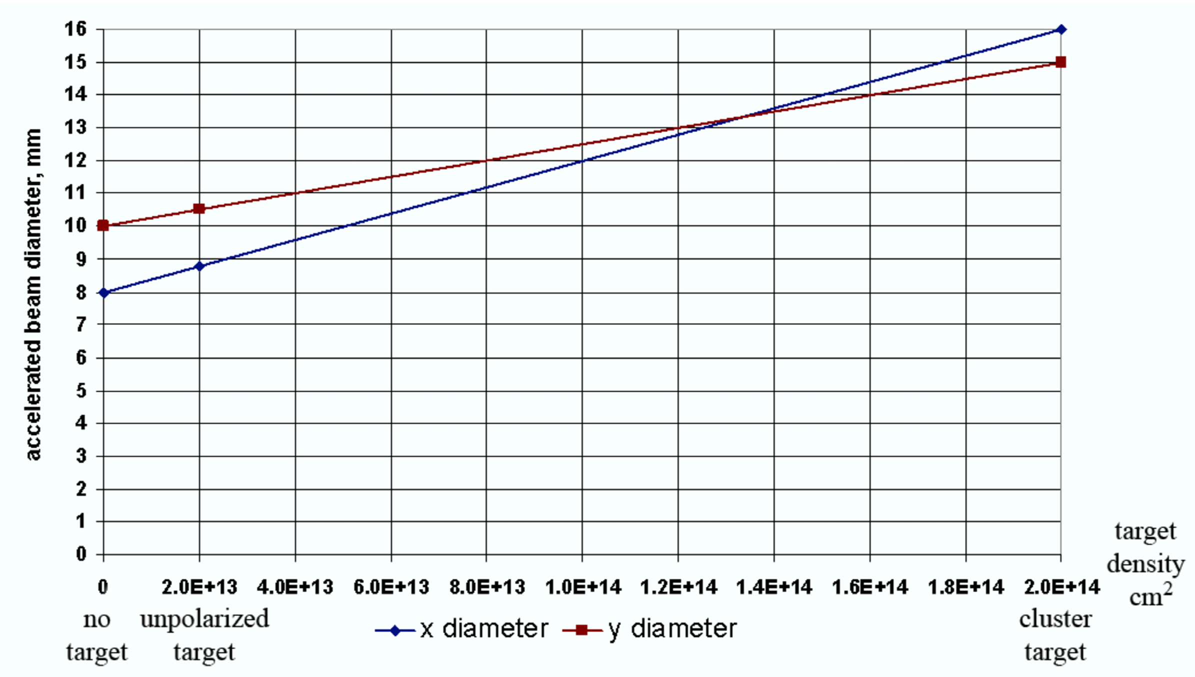

Figure 18: Vertical and horizontal beam dimensions based on the measured target density dependence.

The beam diameter estimated from Fig. 18 (for the case of unpolarised target) and the new cells dimensions are shown in Table 5.

System axes	X [mm]	Y [mm]	Z [mm]
Beam diameter	8.8	10.5	300-400
Cell 1	10	12	350
Cell 2	15	20	350

Table 5: Estimated beam dimensions and the cell sizes for the next tests.

The size in the Z–direction should take into consideration the other equipment installed at ANKE. In order to build an unpolarised gas target, the Unpolarised Gas Supply System (UGSS) can be used. This is available in our laboratory and was already used for the compression tube measurements [26]. The UGSS is used to feed any volume (in our case the storage cell) with a known flux of gas. The type of gas can be changed quickly. In the past, e.g. at PINTEX, injection of unpolarised nitrogen gas was used to determine quantitatively the background from the walls of a storage cell target.

7.5 Request for 1 week beam time for cell tests

We request for one week of beam time for a measurements of CE-break-up with an unpolarised storage cell gas target at $T_d = 1.2$ GeV.

8 Total Requested Beam Time

We ask for THREE weeks of beam time for the charge-exchange and associated measurements at the THREE energies: $T_d = 1.8$, 2.0, and 2.2 GeV with polarisation export [27] from the polarimetry energy of T_d= 1.2 GeV. These energies have been modified slightly compared to our original proposal in order to allow the 1.8 GeV data to be used for the study of the $p(\vec{d},\, ^3\mathrm{He})\eta$ reaction near threshold. Furthermore, there are some data available on the $(\vec{d}, 2p)$ reaction at 2 GeV with which it will be useful to compare. In addition to this physics experiment, we request ONE week for the cell tests discussed above.

References

[1] J. Bystricky et al., Nucl. Phys. A444 (1985) 597.

[2] R.A. Arndt et al., Phys. Rev. C62 (2000) 034005.

[3] M. Altmeier et al., Phys. Rev. Lett. 85 (2000) 1819.

[4] R.A. Arndt et al., Phys. Rev. C50 (1994) 2731; C56 (1997) 3005.

[5] A. de Lesquen et al., Eur. Phys. J C11 (1999) 69.

[6] D.V. Bugg and C. Wilkin, Phys. Lett. B152 (1985) 37.

[7] D.V. Bugg and C. Wilkin, Nucl. Phys. A467 (1987) 575.

[8] A. Kacharava et al., 'The polarised charge-exchange reaction', COSY proposal # 125, Spokesperson: A. Kacharava, F. Rathmann (2003).

[9] S. Barsov et al., Nucl. Instr. Meth. A462 (2001) 364.

[10] S. Barsov et al., submitted to Nucl. Instr. Meth.

[11] V. Komarov et al., Phys. Lett. B553 (2003) 179.

[12] C. Kerboul, Phys. Lett. 181B (1986) 28.

[13] K. Yonehera et al., AIP Conf. Proc. 698 (2003) 763.

[14] N. Katayama et al. Nucl. Phys. A438 (1985) 685.

[15] M. Marshak et al., Phys. Rev. C18 (1978) 1.

[16] G. Korolev et al., Phys. Lett. 165B (1985) 4.

[17] V. Glagolev et al., VII Symposium on Spin Phenomena, Protvino, Sept.86, 1987, p.146 (JINR preprint P1-88-6)

[18] J. Arvieux et al., Nucl. Instr. Meth. A273 (1988) 48.

[19] J. Arvieux et al., Nucl. Phys. A431 (1984) 613.

[20] G.C. Ohlsen, Rep. Prog. Phys. 35 (1972) 717.

[21] J.L. Friedes et al., Phys. Rev. Lett. 15 (1965) 38.

[22] V.V. Glagolev et al., Eur. Phys. J. A15 (2002) 471.

[23] M. Mikirtytchiants et al., Proc. of Int. Workshop on Polarized Sources and Targets, Nashville, Indiana, USA, 2001. ISBN 981-02-4917-9, p. 47.

[24] V. Nelyubin, Proc. of Workshop on Proton–deuteron interaction studies, A. Kacharava, V. Komarov, and F. Rathmann (eds.), Berichte des Forschungszentrum Jülich, 4012. ISSN 0944–2952, p. 189.

[25] SAID database, `http://gwdac.phys.gwu.edu/analysis/nn_analysis.html` .

[26] M. Nekipelov, *Device for Absolute Atomic Beam Intensity Measurements at the ANKE Atomic Beam Source*, Diploma Thesis

[27] R.E. Pollock et al., Phys. Rev. E55 (1997) 7606.